

TITLE: Mycobacteria-induced anaemia revisited: a molecular approach reveals the involvement of NRAMP1 and lipocalin-2, but not of hepcidin.

SHORT TITLE: Hepcidin-independent anaemia of infection.

AUTHORS:

Pedro N. Rodrigues¹⁻², Sandro S. Gomes¹, João V. Neves¹, Sandra Gomes-Pereira¹, Margarida Correia-Neves³, Cláudio Nunes-Alves³, Jens Stolte⁴, Mayka Sanchez⁴, Rui Appelberg¹⁻², Martina U. Muckenthaler⁵ and M. Salomé Gomes¹⁻².

AFFILIATIONS:

1- IBMC- Instituto de Biologia Molecular e Celular, Universidade do Porto, Porto, Portugal

2- ICBAS- Instituto de Ciências Biomédicas Abel Salazar, Universidade do Porto, Porto, Portugal

3- Life and Health Sciences Research Institute (ICVS), School of Health Sciences, University of Minho, Braga, Portugal.

4-European Molecular Biology Lab, Heidelberg, Germany

5- Department of Paediatric Oncology, Haematology and Immunology, University Hospital of Heidelberg, Heidelberg, Germany.

CORRESPONDING AUTHOR:

Maria Salomé Gomes

Address: IBMC- Instituto de Biologia Molecular e Celular da Universidade do Porto;

Rua do Campo Alegre, 823, 4150-180 Porto, Portugal.

Email: sgomes@ibmc.up.pt; phone: +351226074900; fax: +351226099157.

WORD COUNT:

Abstract: 137. Text: 4053.

NUMBER OF FIGURES: 4; NR OF TABLES: 2; NR OF REFERENCES: 45.

PRIMARY SCIENTIFIC CATEGORY: Red Cells, Iron and Erythropoiesis.

Abstract

Anaemia is a frequent complication of chronic infectious diseases but the exact mechanisms by which it develops remain to be clarified. In the present work, we used a mouse model of mycobacterial infection to study molecular alterations of iron metabolism. We show that four weeks after infection with *Mycobacterium avium* BALB/c mice exhibit a moderate anaemia, which cannot be explained by elevated hepatic hepcidin mRNA expression. Instead, the mice respond with increased mRNA expression of *ferroportin (Slc40a1)*, *ceruloplasmin (Cp)*, *hemopexin (Hpx)*, *heme-oxygenase-1 (Hmox1)* and *lipocalin-2 (Lcn2)*. Both the anaemia and the mRNA expression changes of iron-related genes are largely absent in C.D2 mice which bear a functional allele of the *Nramp1* gene. These data suggest that anaemia due to a chronic infection with *M. avium* develops independently of elevated hepcidin expression and possibly involves ferroportin and/or lipocalin-2.

Introduction

Chronic infectious diseases are frequently accompanied by anaemia. It is widely accepted that the anaemia results from the efforts of the host to decrease iron availability for invading microorganisms. Iron retention inside cells of the reticulo-endothelial system has been postulated to be at the basis of this “Iron Withholding System”¹. Macrophages are responsible for the recycling of large amounts of iron, following ingestion and destruction of senescent red blood cells. The iron that is derived from the degradation of haemoglobin is usually released to the circulation in order to be re-utilized in the bone marrow for incorporation into newly forming erythrocytes².

In states of inflammation, the iron recycling process is blocked. Experiments in cells of the mononuclear phagocyte lineage suggest that this may involve LPS-mediated ferroportin-1 down-regulation through a Toll-like receptor 4 (TLR4)-dependent pathway³. In addition, the hepatic iron-regulated peptide hormone hepcidin is highly induced during inflammation. Hepcidin is a key regulator of iron recycling and absorption⁴⁻⁷ which exerts its effect by binding to ferroportin to promote its internalization and degradation⁸. Hepcidin is secreted into the urine of human subjects following injection of LPS, with a peak around 6 h, preceded by an increase in serum IL-6 levels, and followed by a decrease in serum iron⁹. In mice, it has also been shown that the injection of microbial products, such as LPS or complete Freund’s adjuvant (which contains mycobacterial components) lead to the induction of hepcidin mRNA expression in the liver, with maximum values between 1.5 and 16 hours post-treatment¹⁰⁻¹³. When synthetic hepcidin is injected intraperitoneally into mice, a sharp decrease in serum iron was observed, starting 1 h post-treatment and lasting around 48 h¹⁴. Hepcidin has thus been considered a fundamental player in the development of the

anaemia of inflammation and chronic infection. However, all the studies described above are limited to relatively short time frames, more accurately reflecting the course of an acute infection or inflammation than a chronic situation.

Mycobacteria are intracellular pathogens of macrophages, causing insidious long-lasting infections, both in humans and other hosts. Human mycobacterial infections are frequently accompanied by anaemia¹⁵⁻¹⁷. More than twenty years ago, Marchal and Milon have shown that mice infected with *Mycobacterium bovis* BCG (BCG) developed anaemia, which was most severe at 4 weeks post-infection. These authors have shown that BCG-induced anaemia was T-cell dependent and resulted from decreased erythropoiesis¹⁸⁻¹⁹. At the time of these studies, hepcidin, ferroportin, and several other proteins involved in iron metabolism had not been described. Interestingly, these authors observed that the degree of anaemia induced by mycobacterial infection depended on the mouse strain, being more severe in C57BL/6 than in C3H/He mice¹⁹. These two mouse strains differ, among many other genes, in the *Nramp1* allele. *Nramp1* (Natural Resistance-Associated Macrophage Protein 1, also known as Solute Carrier Family 11, Member a1 or Slc11a1) was discovered as a crucial mouse gene determining resistance or susceptibility to several intracellular pathogens, present in a locus previously known as *Bcg*, *Lsh* or *Ity*²⁰. Its high homology with *Nramp2/DMT1/DCT1/Slc11a2*, a known iron transporter, as well as several functional studies, indicate that NRAMP1 is a proton-coupled divalent cation transporter, capable of transporting Fe²⁺, as well as Mn²⁺ and Zn²⁺²¹. Unlike NRAMP2, however, NRAMP1 is present exclusively in cells of the myeloid lineage (namely neutrophils, macrophages and dendritic cells), in the membranes of lysosomal vesicles²¹. NRAMP1 may contribute to the host defence against infection by a multitude of mechanisms, ranging from element starvation to alterations in phagosome maturation, the production of

reactive oxygen and nitrogen intermediates or the modulation of the release of inflammatory mediators²²⁻²³. A role for NRAMP1 in normal iron metabolism has recently been shown. In vitro, *Nramp1* expression was increased in macrophages undergoing erythro-phagocytosis or heme ingestion and the expression of a functional NRAMP1 protein increased the release of iron from these sources²⁴. In vivo, *Nramp1*-deficient mice exhibited decreased capacity to recycle the iron resulting from erythrophagocytosis, showing augmented iron retention in the liver and spleen²⁵.

Here, we characterized the development of anaemia in mice chronically infected with *Mycobacterium avium*. Using two strains of mice expressing different alleles of *Nramp1*²⁶, we identified hepatic iron-related genes whose expression is significantly affected by *M. avium* infection.

Animals, materials and methods

Mice

The BALB/c (NRAMP1-S) and C.D2 (NRAMP1-R) congenic mouse strains were bred and housed at the Instituto de Biologia Molecular e Celular (IBMC) animal facility. The animals were kept inside individually ventilated cages, bearing high efficiency particulate air (HEPA) filters and were fed sterilized food and water *ad libitum*. For the experimental treatments, 8-12 weeks old females were used. All animal experiments were carried out in compliance with the animal ethics guidelines of the institute, and the national and European regulations for the care and handling of laboratory animals.

Bacteria

Mycobacterium avium strain 2447, forming smooth transparent (SmT) colonies, was isolated from an AIDS patient and was a gift from Dr. F. Portaels (Institute of Tropical Medicine, Antwerp, Belgium). Mycobacteria were grown to mid-log phase in Middlebrook 7H9 medium (Difco, Sparks, MD) containing 0.05% Tween 80 (Sigma, St. Louis, MO) at 37°C. Bacteria were harvested by centrifugation, suspended in a small volume of saline containing 0.05% Tween 80, briefly sonicated to disrupt bacterial clumps, diluted and stored in aliquots at -70°C until use.

Experimental iron overload

To induce iron overload, mice were injected intraperitoneally with 10 mg of iron, as iron-dextran (Sigma). Control mice received an equivalent amount of dextran (Sigma) by the same route. Animals were infected two weeks after the iron-dextran treatment.

Iron overload was confirmed by quantifying liver and spleen non-heme iron by the bathophenanthroline method as previously described²⁷.

Experimental infection and quantification of bacterial load in the organs

Mice were infected intravenously, through a lateral tail vein, with 10^6 CFU of *M. avium*. Control animals received the same volume of saline. At the time points of interest, mice were sacrificed and blood and tissues were harvested for the different analysis. For bacterial quantification, the livers and spleens were aseptically collected and homogenized in a 0.05% Tween 80 solution in distilled water. Serial dilutions were plated into Middlebrook 7H10 agar medium and the plates were incubated at 37 °C for 1 week, when the colonies were counted.

Histological analysis

Samples of liver and spleen were fixed in buffered formaldehyde and incorporated in paraffin blocks. Sections were stained by haematoxylin-eosin for general histological characterization. Ferric iron was detected by Perls' blue staining and *M avium* visualized by the Ziehl-Neelsen stain. A Leica DMLB microscope (Leica Cambridge Lda., Cambridge, UK) equipped with a colour CCD (charge-coupled device) camera was used to examine the liver and spleen sections.

Immuno-histochemistry for Lipocalin-2 was performed as previously described²⁸.

Briefly, liver sections (10 µm) were stained with anti-mouse lipocalin-2/neutrophil gelatinase-associated lipocalin (R&D Systems, Minneapolis, MN, USA) at 1:500 dilution as primary antibody. Biotinylated secondary antibody (Vector Laboratories Inc., Burlingame, CA, USA) was used at 1:200 following standard procedures. Slides

were then subjected to Ziehl-Nielsen coloration following standard techniques. Samples were analyzed using an optical microscope (BX61; Olympus).

Haematological Indices

Blood samples were collected by retro orbital bleeding under anesthesia. For the erythroid parameters, blood was harvested in EDTA tubes and Haemoglobin, Red Blood Cells counts, Haematocrit and Mean Corpuscular Volume assessed on a Coulter-S counter (Coulter Electronics).

RNA preparation, microarray analysis and real-time PCR

Liver samples were collected, snap frozen in liquid nitrogen and stored at -80°C . Total RNA was extracted using the QIAGEN (Hilden, Germany) Rneasy Midi Kit according to the manufacturer's specifications.

The microarray analysis was performed as described previously²⁹.

For the real-time PCR quantification, total RNA (2 μg) was transcribed into cDNA, using Moloney Murine Leukemia Virus Reverse Transcriptase (Fermentas, Ontario, Canada) or Superscript II reverse transcriptase (Invitrogen) according to the recommendations of the manufacturer, using random primers or an oligo(dT)18 primer. Each pair of primers was shown not to co-amplify genomic DNA. All reactions were performed in a total reaction volume of 20 μL with iQTM SYBR[®] Green Supermix (Bio-Rad Laboratories) or SYBR Green PCR Master Mix (Applied Biosystems) and carried out in the iQTM5 instrument (Bio-Rad Laboratories) or in the Applied Biosystems 7500 Fast Real-Time PCR System.

Baseline thresholds were calculated by the Bio-Rad iQ5 program and the threshold cycles (CT) were used in the $2^{-\Delta\Delta\text{Ct}}$ method, where CT values for target genes were

normalized to expression levels of hprt. Values are reported as n-fold difference relative to the control samples, calculated according to the $2^{-\Delta\Delta Ct}$ method.

Statistical analysis

Statistical analysis was performed using Mann Whitney U test and the results are signed as * $p < 0.05$, ** $p < 0.01$ and *** $p < 0.001$.

Results

1- Infection of BALB/c mice with *M. avium* 2447SmT for four weeks causes moderate anaemia

BALB/c mice are naturally susceptible to *M. avium* and develop a chronic and progressive infection following intravenous inoculation with strain 2447SmT³⁰. We thus infected BALB/c mice with 10⁶ CFU of *M. avium* 2447SmT i.v. Four weeks later, the mice were sacrificed and blood was collected for haematological analysis. As shown in Figure 1, *M. avium*-infected BALB/c mice had significant reductions in haemoglobin concentration, red blood cells number and hematocrit, as compared to uninfected animals of the same strain. The mean corpuscular volume was not affected by infection (not shown).

2- *M. avium* infection leads to alterations of iron distribution in tissues.

Anaemia of chronic infection is usually considered to result from iron sequestration inside tissue macrophages. In order to understand if *M. avium* infection in BALB/c mice leads to alterations of iron distribution in infected tissues, we analysed liver and spleen sections after Perl's staining.

We could not detect any significant alterations on liver iron distribution induced by *M. avium* infection. In both uninfected and infected mice, iron staining was found only rarely inside Kupffer cells. No iron deposits could be detected inside other cell types (Figure 2, A and B). Despite undetectable changes in hepatic iron distribution, we observed a significant reduction (nearly 30%) of H- and L-Ferritin levels following infection with *M. avium* (Figure 2, C).

In contrast to the liver, iron levels were clearly decreased in the red pulp of the spleen of infected mice, as compared to uninfected controls (Figure 2, D and E). Conversely, iron accumulation could be seen in spleen areas of bacterial proliferation and cell infiltration, predominantly in the white pulp (Figure 2, E). L-ferritin content in the spleen of *M. avium*-infected mice was reduced by 80% compared to the uninfected animals, while H-ferritin remained unchanged (Figure 2, F).

3- *M. avium* infection alters hepatic expression of iron-related genes

To investigate the mechanisms responsible for the altered iron status associated with *M. avium* infection, we analyzed liver gene expression of iron-related genes using a specialized microarray platform, the “Iron Chip”-version 8. This platform includes 451 genes related to iron metabolism. Of these, 70 genes have shown a variation of at least 30% in their expression levels after *M. avium* infection in BALB/c mice. Table 1A presents the expression changes observed in those genes most directly involved in iron metabolism. The complete microarray data set is available as supplementary material.

We detected differential expression of genes involved in heme metabolism, including a decrease of *Alas1* (aminolevulinic acid synthase 1), a gene involved in heme biosynthesis and increased expression of *Hpx* (hemopexin) and *Hmox1* (heme oxygenase 1), genes involved in heme binding and degradation, respectively.

Additionally, the expression of *Tfrc* (transferrin receptor 1) was decreased and the expression of *Slc40a1* (ferroportin) and *Cp* (ceruloplasmin) was increased. The gene encoding lipocalin-2 (*Lcn2*), a granulocyte-derived peptide involved in bacterial iron sequestration, was the gene that exhibited the highest induction, with a 14-fold increase

in expression. Surprisingly, the expression of genes coding for Interleukin-6 or hepcidin were not significantly altered.

4- Lipocalin-2 but not hepcidin is induced at early time-points of *M. avium* infection.

Because of the importance attributed to hepcidin in regulating iron metabolism upon infection we investigated the kinetics of its expression during the infection process with *M. avium*. At 1, 15, 30 and 60 days post-infection, the relative mRNA expression levels of hepcidin were quantified in the liver. Hepcidin mRNA expression remained unchanged at every time point studied. In contrast, investigation of lipocalin-2 mRNA levels in the same liver samples showed a significant increase with infection, starting on day 1 (3-fold increase) and peaking at 30 days (49-fold increase) of infection, with a decline at day 60 (14-fold increase) (Table 2).

To further characterize the significance of *Lcn2* induction following *M. avium* infection, we determined its immuno-localization in liver sections as shown in Figure 3. We could barely detect lipocalin-2-positive cells in uninfected mouse livers. Starting from day 1 of infection, some isolated cells with strong staining for lipocalin-2 appeared. Based on morphological characteristics, and consistent with lipocalin-2 staining, most of these cells could be identified as polymorphonuclear neutrophils (PMN). At later infection time-points, granulomas developed at the sites of bacterial proliferation. While lipocalin-2 staining was not detectable within the infected cells, many lipocalin-2-positive cells were detectable at the outer border of the granulomas. Most of these cells seemed to be neutrophils. Additionally, some hepatocytes also stained positive for lipocalin-2 (Figure 3) at these later infection time-points.

5- In *M. avium*-infected C.D2 (*Nramp1*-R) mice anaemia and differential mRNA expression of iron-related genes is largely absent

To investigate to what extent *Nramp1* affects the iron-related response to chronic infection, we made use of C.D2 mice, which are congenic with BALB/c, but express the functional allele of *Nramp1* and are naturally resistant to *M. avium*. C.D2 mice were infected with *M. avium* as described above. As expected, four weeks after infection, C.D2 mice had lower bacterial loads than BALB/c in the liver and spleen (Figure 4, A). Furthermore, we could see no differences in infected versus uninfected C.D2 mice, regarding haemoglobin concentration, red blood cell numbers or the haematocrit (data not shown).

In order to understand if this lack of alterations of haematological parameters was reflected on the gene expression profile, we performed microarray analysis using the “Iron Chip” platform with total liver RNA. Differential expression of iron-related genes was significantly reduced in C.D2, compared to the congenic BALB/c mice: only 12 genes revealed at least 30% variation. Overall, the genes whose expression was altered due to infection in C.D2 mice were the ones that showed the highest variation in BALB/c mice (Table 1A and Supplementary material). This suggests that the number of genes and extent of regulation might be directly correlated to the bacterial loads in infected livers. However, some notable exceptions were observed, namely *Hsp105* and *Alas1*, which were regulated in opposite directions in the two mouse strains (Table 1A and Supplementary material).

We have previously shown that C.D2 mice subjected to secondary iron overload are more susceptible to infection by *M. avium*. As a consequence, their bacterial loads in the liver were similar to those found in BALB/c³¹. We thus investigated whether the haematological response of C.D2 mice to infection by *M. avium* was similar to that of

BALB/c mice, once the bacterial load was increased. To that purpose and since iron overload by itself affects the expression of these genes, we compared gene expression profiles of infected versus uninfected BALB/c or C.D2 mice, both in conditions of experimental iron overload induced by one injection i.p. of 10 mg of iron (as iron-dextran) two weeks prior to infection.

As shown in Figure 4 A and B, upon iron-overload bacterial loads in C.D2 increase to levels similar to those found in BALB/c. Nevertheless, the degree of anaemia induced by infection was lower in C.D2 than in BALB/c (Figure 4C). Additionally, in the situation of iron overload, *M. avium* infection resulted in the altered expression of 101 iron-related genes by at least 30% in BALB/c mice, whereas in C.D2, only 57 genes were similarly regulated. Notably, heme-oxygenase 1, hemopexin, and lipocalin-2 were up-regulated 2 fold or more in BALB/c, whether or not previously iron-loaded, but were not significantly regulated in C.D2 mice (Table 1). Interestingly, in the situation of iron overload, *M. avium* infection led to a reduction in hepcidin expression, both in BALB/c and C.D2 mice.

Discussion

In this work, we present a molecular characterization of the anaemia induced by chronic mycobacterial infection in the mouse. We show that mice infected with *M. avium* exhibit a moderate, normocytic anaemia, at the beginning of the chronic phase of infection, a finding consistent with previous reports¹⁸. The anemia is hallmarked by decreased red blood cell counts, haemoglobin values and hematocrit (Figure 1). In addition, tissue iron distribution is changed towards the accumulation of iron inside macrophages. Most of the observed physiological changes would be compatible with elevated hepcidin expression, yet unexpectedly hepatic hepcidin levels remain unaltered.

Given the central role played by the liver in the regulation of both the inflammatory process and iron metabolism, we used a microarray approach to investigate hepatic mRNA expression of iron-related genes. Several genes that exhibit significant regulation as a consequence of *M. avium* infection code for the known “acute phase reactants” such as ceruloplasmin and hemopexin. We have also found significant induction of several metallothioneins, similarly to previous findings in LPS injected mice³². In contrast, mRNA expression of other acute phase proteins such as transferrin, ferritin, and hepcidin, which were previously shown to be regulated in response to LPS¹² remain unchanged. These findings suggest that chronic infection activates a genetic program that differs from that of acute inflammation and has a distinct impact on iron metabolism. Interestingly, our results also differ from those obtained in other (non-infectious) models of chronic inflammation. For example, rats with chronic arthritis accompanied by anaemia showed no change in the liver mRNA expression of Transferrin receptor 1 or Ferroportin, but showed significant increases in the expression of DMT1 and Hepcidin³³.

It thus seems that each defined infectious or inflammatory condition induces a different response in terms of iron metabolism. One of the most relevant observations made in this work is that chronic mycobacterial infection leads to anaemia independently of the induction of hepcidin, implying that alternative mechanisms must operate to lead to iron re-distribution and anaemia in this particular setting.

Consistent with our previously reported data in Hfe-deficient mice³⁴, BALB/c mice infected with *M. avium* accumulate iron within hepatic and splenic infected macrophages, right at the centre of granulomatous lesions (Figure 2). This observation suggests that upon mycobacterial infection iron is re-distributed into macrophages which may cause iron depletion in the organ parenchyma. Relative iron deficiency in cell types other than macrophages may explain the overall decrease in H- and L-ferritin protein levels both in the liver and the spleen of *M. avium* infected mice. In addition, we saw a decrease in the expression of *transferrin receptor 1* and increases in the expression of *ferroportin* and *ceruloplasmin*, which together may contribute to the decrease of intracellular iron accumulation by hepatocytes. Concurrent decreases in TfR1 mRNA and ferritin protein suggests that these responses are uncoupled from the IRE/IRP regulatory system. How these responses are triggered and whether macrophage iron accumulation is an efficient host strategy to combat infection or a process that favours *M. avium* growth is currently unknown.

The hepatic iron-related gene that showed the highest induction in response to *M. avium* infection was lipocalin-2 (*Lcn2*). Increased lipocalin-2 expression was further confirmed at the protein level by immuno-histochemistry on liver sections. Interestingly, staining for lipocalin-2 was not detected inside infected macrophages but rather inside polymorphonuclear neutrophils and also inside hepatocytes, at later time-points. These

observations are in line with previous reports in which lipocalin-2 staining was found predominantly in endothelial cells (and not macrophages) of mice aerogenically infected with mycobacteria, despite the fact that alveolar macrophages strongly up-regulated *Lcn2* expression when infected with mycobacteria in vitro³⁵. Strong staining for lipocalin-2 has also been observed in the hepatocytes of mice infected intraperitoneally with *Escherichia coli*³⁶. Overall, these observations suggest that during infection different cell types may contribute to the production and release of lipocalin-2. Interestingly, neutrophils are important producers of lipocalin 2, but its synthesis is thought to occur at the earlier steps of neutrophil differentiation in the bone marrow, and no *Lcn2* mRNA is detectable in mature circulating or inflammatory neutrophils³⁷. It is thus not clear whether the increase in *Lcn2* mRNA levels induced by *M. avium* in our model is mainly contributed by neutrophils or other cell types.

Lipocalin-2 can bind carboxymycobactin, a mycobacterial siderophore³⁸ and inhibit growth of *Mycobacterium tuberculosis* and *M. bovis* in liquid culture^{35,39}. Additionally, mice genetically deficient in lipocalin-2 have increased susceptibility to pulmonary tuberculosis³⁵. Our work does not address a possible role for lipocalin-2 in resistance against *M. avium*. However, our data indicate that this peptide is not a determinant factor for resistance to this infection since the mouse strain which exhibits a higher *Lcn2* induction (BALB/c) is also the one which allows a more extensive bacterial proliferation.

Lipocalin-2 has been shown to decrease erythropoiesis in vitro⁴⁰. It's possible involvement in the development of anaemia in response to *M. avium* remains to be determined in future experiments using lipocalin-2-deficient mice. Since *Lcn2* was also reported to be up-regulated by anaemia⁴¹ it is also possible that the increase in *Lcn2* is a consequence of the mycobacteria-induced anaemia. This explanation is however rather

unlikely, since significant induction of *Lcn2* was detectable as early as 24 h after *M. avium* infection (Table 2), a time at which we did not observe any alteration on haematological parameters (data not shown).

Interestingly, induction of *Lcn2* in the liver, after infection with *M. avium*, was *Nramp1*-dependent. The difference in *Lcn2* induction between mouse strains seemed independent of bacterial loads (Table 1 and Figure 4). It is thus tempting to speculate that *Nramp1* expression may directly affect lipocalin-2 production. NRAMP1 is expressed exclusively in cells of myeloid origin including neutrophils and its sub-cellular localization may even be partially overlapping with that of lipocalin-2^{37,42}. Alternatively, *Nramp1* expression and function may affect *Lcn2* expression indirectly, through the modulation of cytokine production.

Nramp1^{+/+} mice show a more pronounced inflammatory response than *Nramp1*^{-/-} mice at early time-points of infection, with increased production of pro-inflammatory cytokines and a higher recruitment of neutrophils and macrophages⁴³⁻⁴⁴. We cannot exclude the possibility that in our model there is a difference in the kinetics of anaemia development between BALB/c and C.D2 mice.

A role for NRAMP1 in normal iron metabolism has been predicted for a long time. Recently, Soe-Lin et al, using the 129Sv mouse strain, have shown that the disruption of the *Nramp1* gene resulted in a significant and progressive increase in the spleen iron content as mice age²⁵. Accordingly, when we compared the spleen iron contents of C.D2 (which carry a functional allele of *Nramp1*) and BALB/c (which have the mutated form of *Nramp1*) uninfected mice, we have consistently found lower levels in the former, but these differences did not reach statistical significance (data not shown), possibly due to differences in basal iron levels between these strains and 129Sv. NRAMP1 was also shown to influence the way mice deal with iron in abnormal

situations^{25,45}. After acute or chronic haemolytic anaemia, *Nramp1*-deficient mice were less capable of recovering normal haematological parameters than wild-type controls and instead accumulated iron in the tissues where erythrophagocytosis predominantly occurs, namely the spleen²⁵. These observations are consistent with our findings that *Nramp1*-deficient mice develop a more severe anaemia after chronic infection than mice carrying a functional allele of this protein and suggest that NRAMP1 plays a critical role in iron recycling, by facilitating the release of haemoglobin-derived iron for an efficient reutilization.

The impact of *M. avium* infection on iron distribution and processing in the spleen, namely on erythrophagocytosis and iron recycling, will be detailed in future studies.

Extensive and important progress has occurred in recent years in the understanding of the molecular mechanisms of the regulation of iron metabolism. One of the most challenging areas of research in this context is anaemia of chronic infection. It would be of much clinical interest to try to correct host anaemia without a risk of increasing iron availability to the pathogen. With that purpose, it is mandatory to better understand the circuits of regulation of iron metabolism during chronic infection. With this work, we found that anaemia of chronic infection can develop without the significant induction of hepcidin and we identified lipocalin-2 and NRAMP1 as possible important players in this process. The infection model presented here can be a valuable tool to achieve further progress in this area.

Acknowledgements:

This work was supported by the EEC Framework 6 (LSHM-CT-2006037296

EuroIron1) and FCT-approved grant POCTI/MGI/40132/2001, funded by FEDER.

Authorship: P.N.R. and M.S.G. designed the experimental work. P.N.R., S.S.G., J.V.N., S.G.P., C.N.A., J.S., M.S.G. performed experimental work. P.N.R., M.C.N., R.A., M.U.M. and M.S.G. analysed the data. M.S.G. wrote the paper, with contributions from P.N.R., M.C.N., M.S., R.A. and M.U.M.

Conflict of interests disclosure: The authors declare no competing financial conflict of interests.

References

1. Weinberg ED. Iron depletion: a defense against intracellular infection and neoplasia. *Life Sci.* 1992;50:1289-1297.
2. Knutson M, Wessling-Resnick M. Iron metabolism in the reticuloendothelial system. *Crit Rev Biochem Mol Biol.* 2003;38:61-88.
3. Yang F, Liu XB, Quinones M, Melby PC, Ghio A, Haile DJ. Regulation of reticuloendothelial iron transporter MTP1 (Slc11a3) by inflammation. *J Biol Chem.* 2002;277:39786-39791.
4. Andrews NC. Anemia of inflammation: the cytokine-hepcidin link. *J Clin Invest.* 2004;113:1251-1253.
5. Ganz T. Molecular pathogenesis of anemia of chronic disease. *Pediatr Blood Cancer.* 2006;46:554-557.
6. Hentze MW, Muckenthaler MU, Andrews NC. Balancing acts: molecular control of mammalian iron metabolism. *Cell.* 2004;117:285-297.
7. Weiss G. Iron metabolism in the anemia of chronic disease. *Biochim Biophys Acta.* 2009;1790:682-693.
8. Nemeth E, Tuttle MS, Powelson J, et al. Heparin regulates cellular iron efflux by binding to ferroportin and inducing its internalization. *Science.* 2004;306:2090-2093.
9. Kemna E, Pickkers P, Nemeth E, van der Hoeven H, Swinkels D. Time-course analysis of hepcidin, serum iron, and plasma cytokine levels in humans injected with LPS. *Blood.* 2005;106:1864-1866.

10. Constante M, Jiang W, Wang D, Raymond VA, Bilodeau M, Santos MM. Distinct requirements for Hfe in basal and induced hepcidin levels in iron overload and inflammation. *Am J Physiol Gastrointest Liver Physiol.* 2006;291:G229-237.
11. Frazer DM, Wilkins SJ, Millard KN, McKie AT, Vulpe CD, Anderson GJ. Increased hepcidin expression and hypoferraemia associated with an acute phase response are not affected by inactivation of HFE. *Br J Haematol.* 2004;126:434-436.
12. Pigeon C, Ilyin G, Courselaud B, et al. A new mouse liver-specific gene, encoding a protein homologous to human antimicrobial peptide hepcidin, is overexpressed during iron overload. *J Biol Chem.* 2001;276:7811-7819.
13. Roy CN, Custodio AO, de Graaf J, et al. An Hfe-dependent pathway mediates hyposideremia in response to lipopolysaccharide-induced inflammation in mice. *Nat Genet.* 2004;36:481-485.
14. Rivera S, Nemeth E, Gabayan V, Lopez MA, Farshidi D, Ganz T. Synthetic hepcidin causes rapid dose-dependent hypoferremia and is concentrated in ferroportin-containing organs. *Blood.* 2005;106:2196-2199.
15. Hasibi M, Rasoulinejad M, Hosseini SM, Davari P, Sahebain A, Khashayar P. Epidemiological, clinical, laboratory findings, and outcomes of disseminated tuberculosis in Tehran, Iran. *South Med J.* 2008;101:910-913.
16. Maartens G, Willcox PA, Benatar SR. Miliary tuberculosis: rapid diagnosis, hematologic abnormalities, and outcome in 109 treated adults. *Am J Med.* 1990;89:291-296.
17. Muzaffar TM, Shaifuzain AR, Imran Y, Haslina MN. Hematological changes in tuberculous spondylitis patients at the Hospital Universiti Sains Malaysia. *Southeast Asian J Trop Med Public Health.* 2008;39:686-689.

18. Marchal G, Milon G. Decreased erythropoiesis: the origin of the BCG induced anaemia in mice. *Br J Haematol.* 1981;48:551-560.
19. Marchal G, Milon G. Control of hemopoiesis in mice by sensitized L3T4+ Lyt2- lymphocytes during infection with bacillus Calmette-Guerin. *Proc Natl Acad Sci U S A.* 1986;83:3977-3981.
20. Vidal SM, Malo D, Vogan K, Skamene E, Gros P. Natural resistance to infection with intracellular parasites: isolation of a candidate for Bcg. *Cell.* 1993;73:469-485.
21. Courville P, Chaloupka R, Cellier MF. Recent progress in structure-function analyses of Nramp proton-dependent metal-ion transporters. *Biochem Cell Biol.* 2006;84:960-978.
22. Blackwell JM, Searle S, Mohamed H, White JK. Divalent cation transport and susceptibility to infectious and autoimmune disease: continuation of the Ity/Lsh/Bcg/Nramp1/Slc11a1 gene story. *Immunol Lett.* 2003;85:197-203.
23. Cellier MF, Courville P, Champion C. Nramp1 phagocyte intracellular metal withdrawal defense. *Microbes Infect.* 2007;9:1662-1670.
24. Soe-Lin S, Sheftel AD, Wasyluk B, Ponka P. Nramp1 equips macrophages for efficient iron recycling. *Exp Hematol.* 2008;36:929-937.
25. Soe-Lin S, Apte SS, Andriopoulos B, Jr., et al. Nramp1 promotes efficient macrophage recycling of iron following erythrophagocytosis in vivo. *Proc Natl Acad Sci U S A.* 2009;106:5960-5965.
26. Potter M, O'Brien AD, Skamene E, et al. A BALB/c congenic strain of mice that carries a genetic locus (Ityr) controlling resistance to intracellular parasites. *Infect Immun.* 1983;40:1234-1235.

27. Rodrigues P, Lopes C, Mascarenhas C, Arosio P, Porto G, De Sousa M. Comparative study between Hfe^{-/-} and beta2m^{-/-} mice: progression with age of iron status and liver pathology. *Int J Exp Pathol*. 2006;87:317-324.
28. Marques F, Rodrigues AJ, Sousa JC, et al. Lipocalin 2 is a choroid plexus acute-phase protein. *J Cereb Blood Flow Metab*. 2008;28:450-455.
29. Muckenthaler MU, Rodrigues P, Macedo MG, et al. Molecular analysis of iron overload in beta2-microglobulin-deficient mice. *Blood Cells Mol Dis*. 2004;33:125-131.
30. Castro AG, Minoprio P, Appelberg R. The relative impact of bacterial virulence and host genetic background on cytokine expression during *Mycobacterium avium* infection of mice. *Immunology*. 1995;85:556-561.
31. Gomes MS, Appelberg R. Evidence for a link between iron metabolism and Nramp1 gene function in innate resistance against *Mycobacterium avium*. *Immunology*. 1998;95:165-168.
32. Rofe AM, Philcox JC, Coyle P. Trace metal, acute phase and metabolic response to endotoxin in metallothionein-null mice. *Biochem J*. 1996;314 (Pt 3):793-797.
33. Theurl I, Aigner E, Theurl M, et al. Regulation of iron homeostasis in anemia of chronic disease and iron deficiency anemia: diagnostic and therapeutic implications. *Blood*. 2009;113:5277-5286.
34. Gomes-Pereira S, Rodrigues PN, Appelberg R, Gomes MS. Increased susceptibility to *Mycobacterium avium* in hemochromatosis protein HFE-deficient mice. *Infect Immun*. 2008;76:4713-4719.
35. Saiga H, Nishimura J, Kuwata H, et al. Lipocalin 2-dependent inhibition of mycobacterial growth in alveolar epithelium. *J Immunol*. 2008;181:8521-8527.
36. Flo TH, Smith KD, Sato S, et al. Lipocalin 2 mediates an innate immune response to bacterial infection by sequestering iron. *Nature*. 2004;432:917-921.

37. Kjeldsen L, Cowland JB, Borregaard N. Human neutrophil gelatinase-associated lipocalin and homologous proteins in rat and mouse. *Biochim Biophys Acta*. 2000;1482:272-283.
38. Holmes MA, Paulsene W, Jide X, Ratledge C, Strong RK. Siderocalin (Lcn 2) also binds carboxymycobactins, potentially defending against mycobacterial infections through iron sequestration. *Structure*. 2005;13:29-41.
39. Martineau AR, Newton SM, Wilkinson KA, et al. Neutrophil-mediated innate immune resistance to mycobacteria. *J Clin Invest*. 2007;117:1988-1994.
40. Miharada K, Hiroyama T, Sudo K, Nagasawa T, Nakamura Y. Lipocalin 2 functions as a negative regulator of red blood cell production in an autocrine fashion. *FASEB J*. 2005;19:1881-1883.
41. Jiang W, Constante M, Santos MM. Anemia upregulates lipocalin 2 in the liver and serum. *Blood Cells Mol Dis*. 2008;41:169-174.
42. Canonne-Hergaux F, Calafat J, Richer E, et al. Expression and subcellular localization of NRAMP1 in human neutrophil granules. *Blood*. 2002;100:268-275.
43. Appelberg R, Pedrosa JM, Silva MT. Host and bacterial factors control the *Mycobacterium avium*-induced chronic peritoneal granulocytosis in mice. *Clin Exp Immunol*. 1991;83:231-236.
44. Valdez Y, Grassl GA, Guttman JA, et al. Nramp1 drives an accelerated inflammatory response during Salmonella-induced colitis in mice. *Cell Microbiol*. 2009;11:351-362.
45. Biggs TE, Baker ST, Botham MS, Dhital A, Barton CH, Perry VH. Nramp1 modulates iron homeostasis in vivo and in vitro: evidence for a role in cellular iron release involving de-acidification of intracellular vesicles. *Eur J Immunol*. 2001;31:2060-2070.

Table 1- Regulation by *M. avium* infection of liver genes involved in iron metabolism, as determined by the microarray analysis with the “Iron chip”. * Confirmed by quantitative real-time PCR; nr: not significantly altered.

			A- Dextran only		B- Iron -dextran	
			BALB/c	C.D2	BALB/c	C.D2
Tfrc1	*	Transferrin Receptor 1	-2.0	nr	nr	+1.3
Alas1	*	Aminolevulinic acid synthase 1	-1.6	+2.1	-2.4	-2.9
Hamp	*	Hepcidin	nr	nr	-1.8	-1.8
Ltf		Lactoferrin	-1.4	nr	nr	nr
Ftl1		Ferritin L chain 1	nr	nr	nr	-1.7
IL6ra		Interleukin 6 receptor alpha	nr	nr	nr	-1.6
Slc11a2		DCT-1 (NRAMP2) exon 1A	nr	nr	nr	-1.5
Slc11a2		DCT-1 (NRAMP2) exon 1B	nr	nr	+1.4	-1.7
Slc40a1	*	Ferroportin	+1.4	nr	nr	+1.4
Cp	*	Ceruloplasmin	+1.4	nr	+1.5	nr
IL6		Interleukin 6	nr	nr	+1.8	-1.9
Hba-a1		Hemoglobin alpha, adult chain 1	+1.7	+1.5	+2.2	-1.6
Hbb-bh1		Hemoglobin Z, β -like embryonic chain	+1.8	+1.5	+2.3	nr
Hmox1	*	Heme oxygenase 1	+2.1	nr	+2.3	nr
Hpxn	*	Hemopexin	+2.1	nr	+2.3	nr
Lcn2	*	Lipocalin 2	+13.9	+1.4	+9.0	nr
Total number of genes whose expression was altered more than 1.3 times			70	12	101	57

Table 2- Alteration of expression, during *M. avium* infection, of genes involved in iron metabolism, in the livers of BALB/c mice, as determined by real-time PCR. Grey shading corresponds to statistically significant regulation. *Lcn2*, lipocalin 2; *Hamp*, hepcidin.

days	<i>Lcn2</i>			<i>Hamp</i>		
1	3.04	±	0.68	1.19	±	0.39
15	2.46	±	0.47	0.99	±	0.23
30	49.17	±	19.59	0.99	±	0.16
60	14.48	±	11,77	1.07	±	0.20

Figure legends

Figure 1- Alterations on haematological parameters induced by mycobacterial infection.

BALB/c mice were infected i.v. with 10^6 CFU of *M. avium* 2447SmT (black bars) or left uninfected (white bars). Four weeks later, mice were sacrificed and blood was collected for determination of Red Blood Cells count, Haemoglobin concentration and Haematocrit. Values in each graph are the average \pm one standard deviation of 7 mice per group. Mann-Whitney U test was used to compare uninfected and infected groups of mice. ** corresponds to $p < 0.01$.

Figure 2- Impact of *M. avium* infection on tissue iron distribution and ferritin concentration.

BALB/c mice were infected or not with 10^6 CFU of *M. avium* 2447SmT, as described for Figure 1. Four weeks after infection, liver and spleen samples were collected and processed for histological examination. Tissue iron distribution was evaluated by Perl's staining (A and B-liver, D and E- spleen). Asterisks indicate sites of bacterial proliferation with the infiltration of immune cells.

L- and H-ferritin content was measured by ELISA in the livers (C) and the spleens (F) of uninfected (white bars) and *M. avium*-infected mice (black bars). The results are shown as the average \pm one standard deviation of 7 mice per group. Mann-Whitney U test was used to compare uninfected and infected groups. *, $p < 0.05$; **, $p < 0.01$.

Figure 3- Expression of Lipocalin-2 in the livers of *M. avium*- infected mice.

BALB/c mice were infected with 10^6 CFU of *M. avium* 2447SmT. At different time-points after infection, 4 or 5 mice were sacrificed and liver sections were collected for

immuno-cytochemical analysis of lipocalin-2 distribution. Arrows indicate lipocalin-2-positive hepatocytes.

Figure 4- Relative impact of *M. avium* infection on the haematological parameters of BALB/c and C.D2 mice.

Groups of BALB/c and C.D2 mice were i.p. injected with 10 mg of iron (as iron dextran) (B) or dextran alone (A). Two weeks later, mice were infected i.v. with *M. avium* 2447SmT or injected with an equivalent volume of saline. Four weeks after infection, mice were sacrificed and the bacterial loads were quantified in the livers and spleens. The graphs show the geometric mean \pm one standard deviation of log₁₀ CFU/organ of 7 mice per group.

(C) Haematological parameters evaluated four weeks after infection in previously iron loaded BALB/c and C.D2 mice. Mann-Whitney U test was used to compare uninfected and infected groups. *, p<0.05; **, p<0.01.

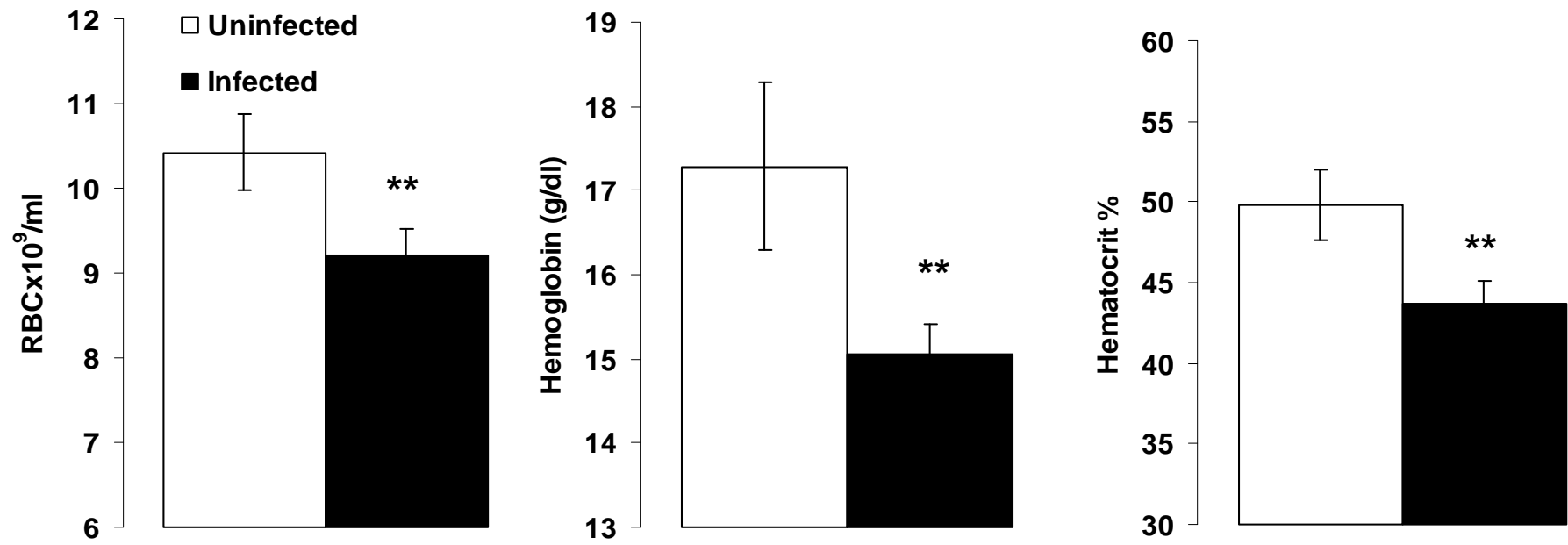


Figure 1

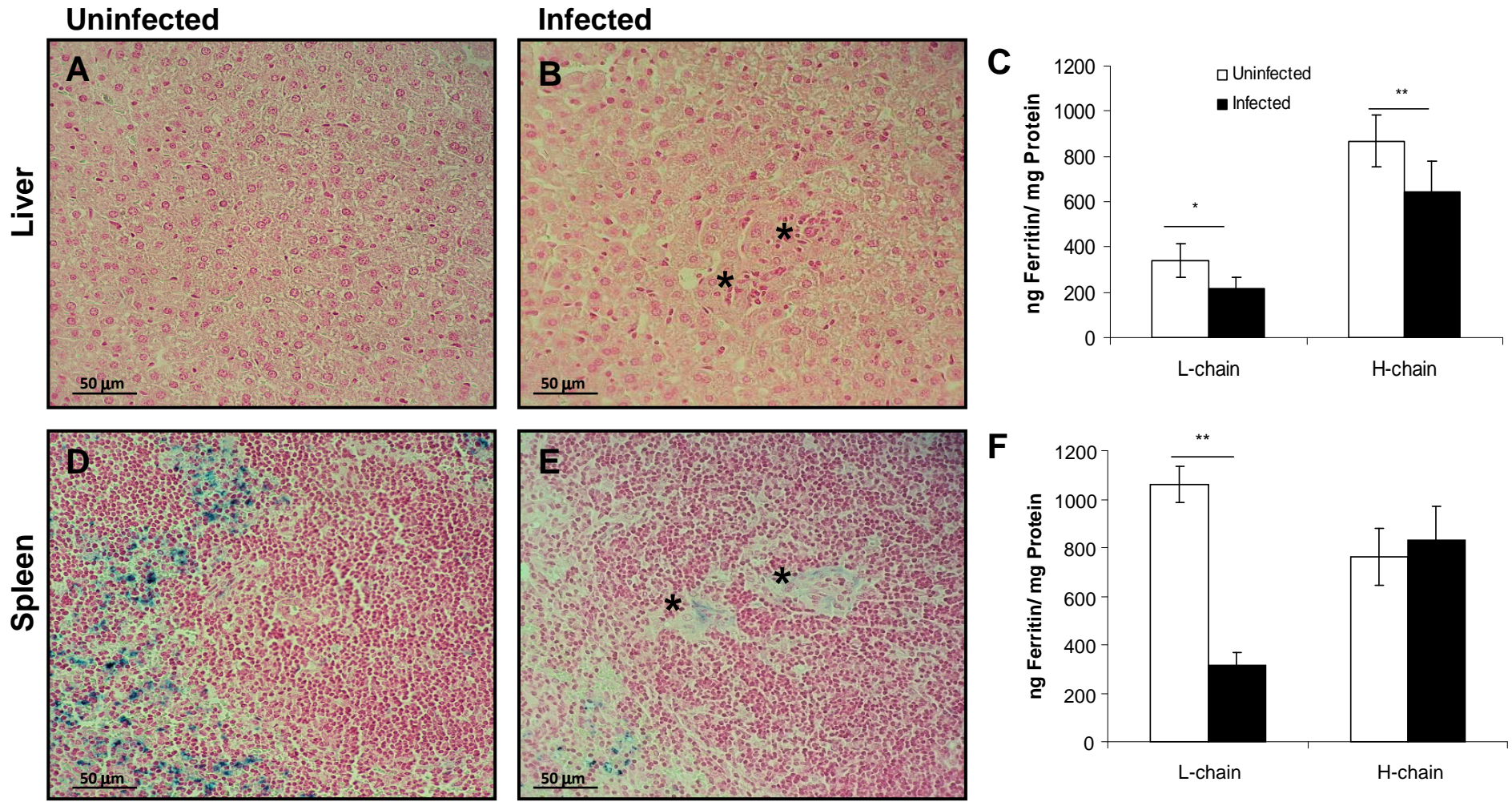
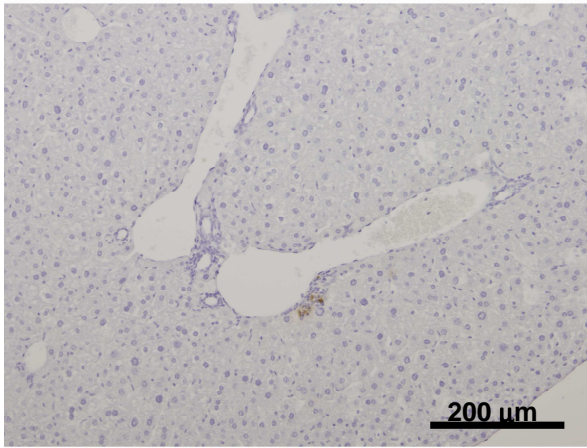
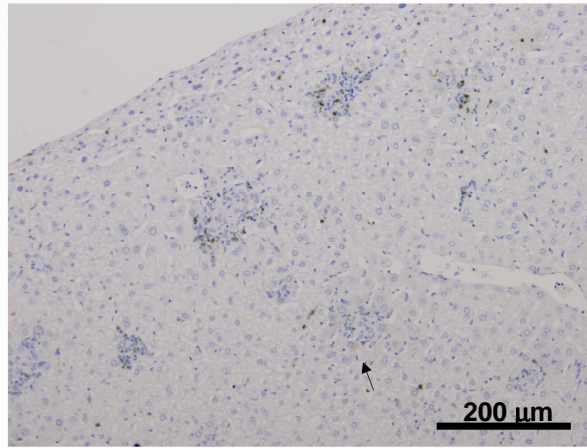


Figure 2

1day



30 days



60 days

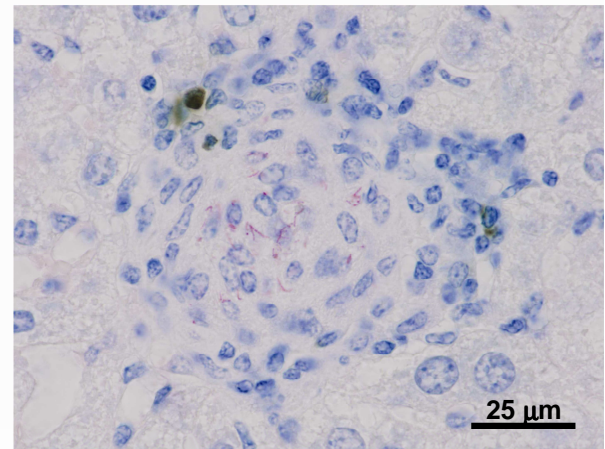
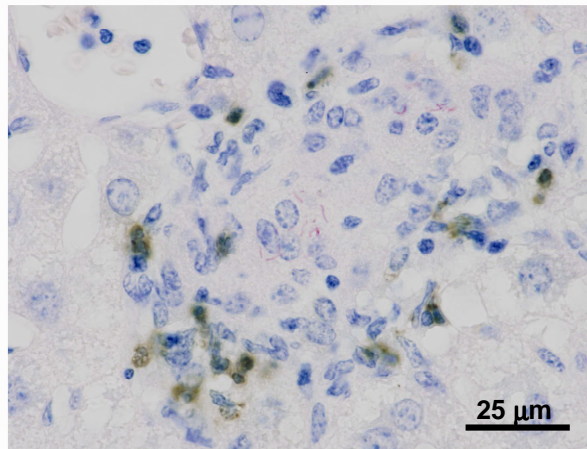
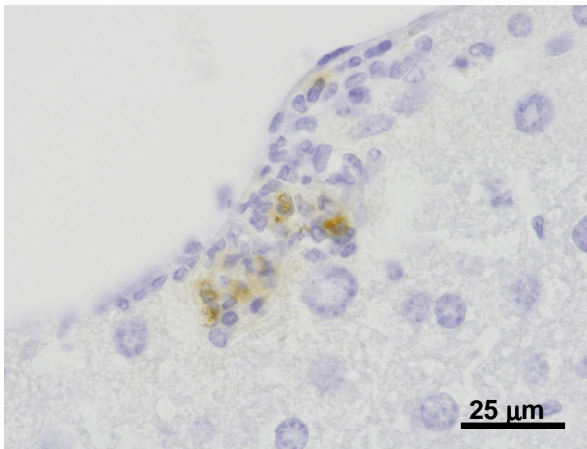
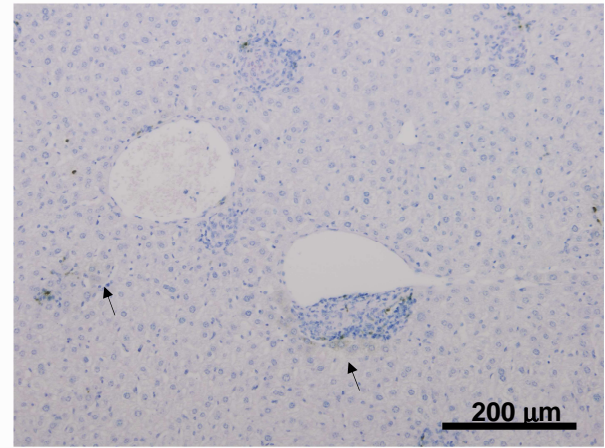


Figure 3

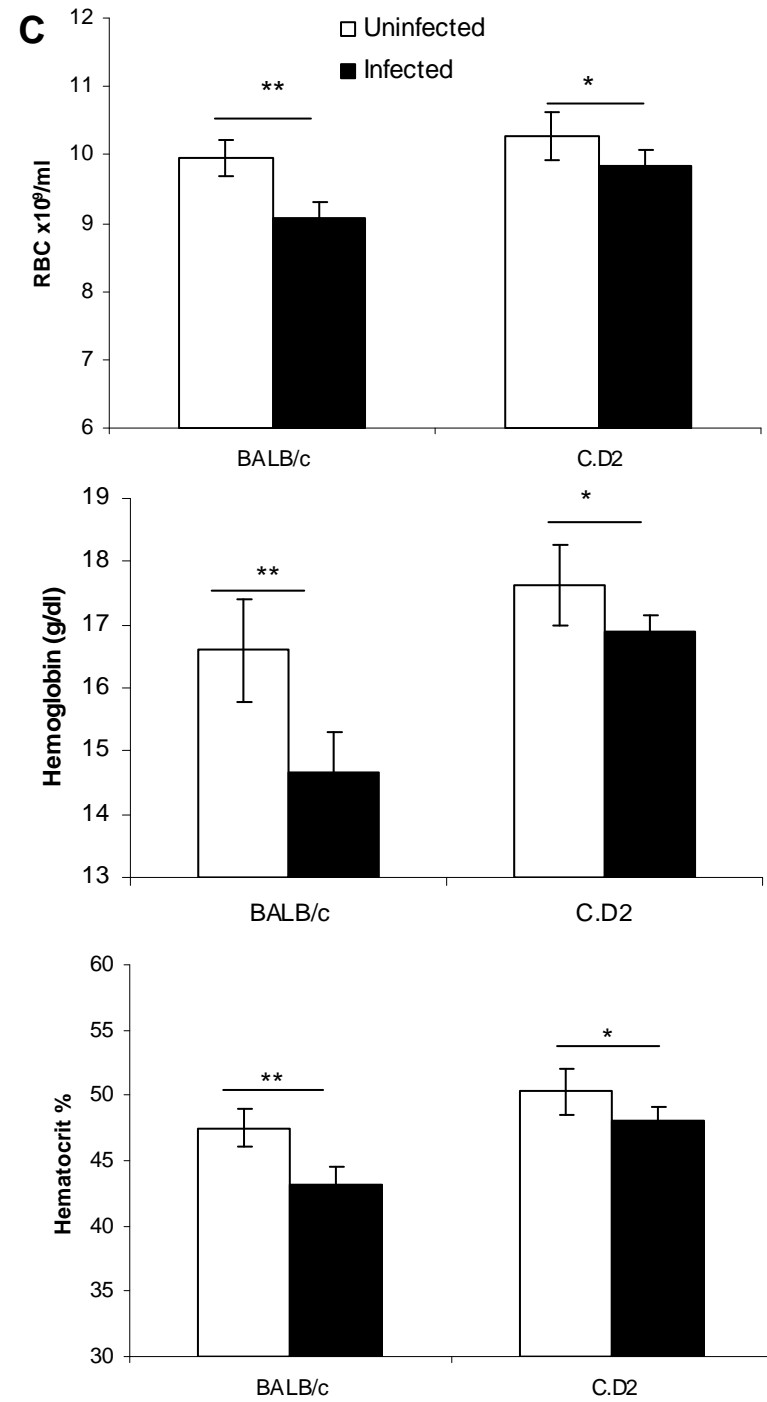
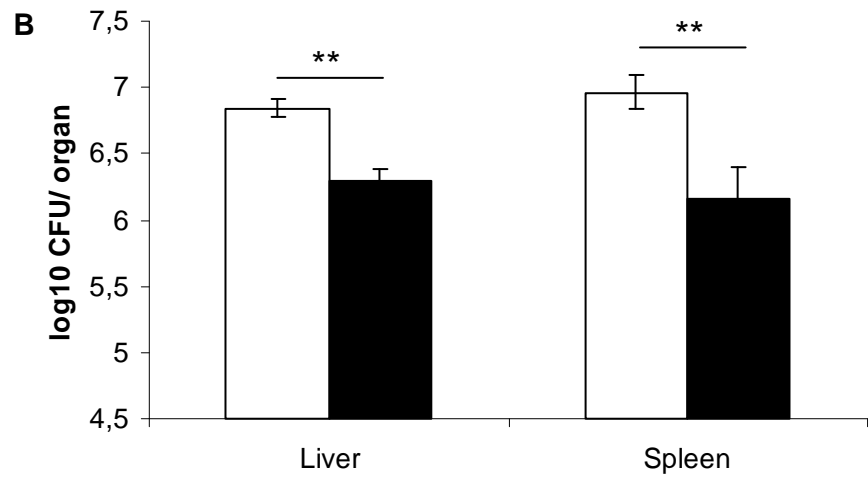
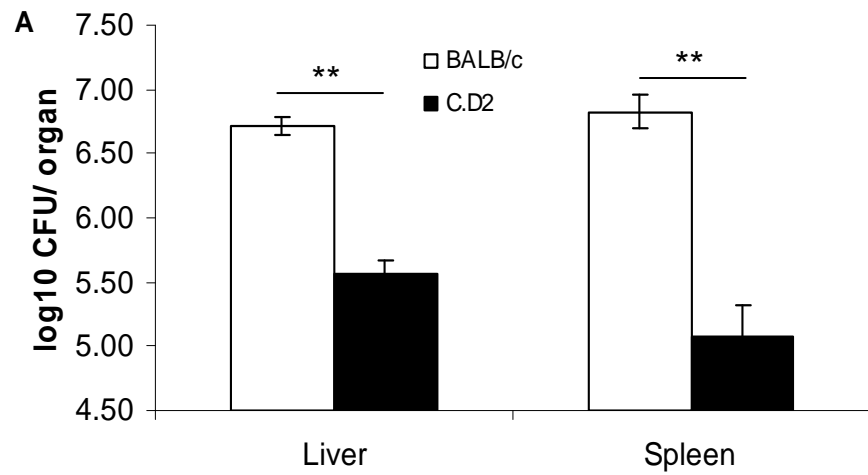


Figure 4